

Effect of coal blending ratio on CO₂ coke gasification

Jin-Ho Kim, Gyeong-Min Kim, Kevin Yohanes Lisandy, and Chung-Hwan Jeon[†]

School of Mechanical Engineering, Pusan Clean Coal Center, Pusan National University, Busan 46241 Korea
(Received 19 March 2017 • accepted 13 July 2017)

Abstract—Coke gasification is largely influenced by the raw coal, catalyst, and blending ratios, pore structure, and specific surface area of the raw coal. In this study, several properties of cokes related to their reactivity were measured using coke reactivity test apparatus (CRTA), scanning electron microscopy (SEM), thermogravimetric analysis (TGA), Brunauer-Emmet-Teller (BET) surface area analysis, and energy dispersive X-ray spectroscopy (EDS) to investigate the characteristics of coke gasification. The results indicated that the reactivity of coke in the temperature range from 950 to 1,050 °C was affected by the type of coke and its specific surface area rather than the general properties of the coke, although the overall reactivities at the other temperatures were uniform. EDS analysis showed that the catalyst acted on the reactivity of cokes at low temperatures, whereas the BET analysis indicated that the reactivity at high temperature was influenced by the specific surface area.

Keywords: CRTA (Coke Reactivity Test Apparatus), Coke, CO₂ Gasification, Pore Development, Catalyst

INTRODUCTION

Blast furnaces are not only a major source of greenhouse gas (GHG) emissions but also consume much energy. To increase the efficiency of blast furnaces, it is necessary to use cokes that are strong enough to maintain the structure of both coke and iron ore, while also having high reactivity toward CO₂ gas to generate a large quantity of CO, a reducing gas [1]. The gasification reaction is a process that produces synthesis gas such as H₂ and CO from carbon, i.e., coal, cokes, heavy residual oil, wastes, and biomass [2,3].

Coke, which has a very high carbon content, is generally produced by destructive distillation of coal in a coke oven. High-quality coke should have low moisture content, low impurities, high strength, relatively low reactivity, and uniform particle size distribution. These properties are mainly affected by the coking condition such as coal type, blending ratio, particle size, bulk density, heating rate and coking temperature.

Coke plays three essential roles—thermal, chemical, and physical—in the steelmaking process with a blast furnace. First, in its thermal role as the source of 60-80% of the energy for the blast furnace, coke supplies sufficient heat to melt iron and slag through an exothermic reaction in the blast furnace. Second, through its chemical role as a reducing agent, coke generates the reducing gases required to reduce iron and other oxides [4], while also playing a role in mixing molten iron in the lower part of the blast furnace with carbon. Finally, its physical role involves withstanding the weight of the material and maintaining the permeability in the lower part of the blast furnace. The permeability of coke controls the gas flow and distribution, as well as the melt flow and release of melting iron in the lower part of the blast furnace.

In relation to blast furnace performance, the effects of analysis

on coke reactivity are not very clear. However, most blast furnace operators claim that coke should not react readily at low temperatures to avoid carbon consumption in the upper part of the furnace where the temperatures are low. Moreover, the highly reactive coke becomes very weak to the point that it cannot support the burden while the burden travels to the lower portion of the blast furnace. There have been numerous studies on the reactivity and strength of coke [6,9,12].

The factors that affect the reactivity of coke include texture (carbon forms), structure (porosity, pore size, pore wall thickness), ash composition (alkalis, sulfur, iron) etc. [5-7]. Isotropic textured coke obtained from weak coking of highly volatile (HV) coal becomes chemically weak due to the gasification reaction with CO₂. Conversely, coking HV and medium volatile (MV) coal produce coarse, circular, and lenticular carbon-type cokes with low reactivity, while the low volatile (LV) coal produces ribbon-like carbon type coke with medium reactivity [10,11].

As the porosity of coke increases, its reactivity also increases [8, 15]. When different ranks and types of coal are carbonized, they produce different coke structures after gasification. Coke produced from low-rank HV coal shows the characteristics of thicker walls and smaller pore areas [9].

Accordingly, we used a coke reactivity test apparatus (CRTA), designed to simulate coke gasification inside a blast furnace, for comparative analysis of the reactivity of coke. The level of reactivity was assessed based on the concentration of CO gas emitted after CO₂ gasification using various reaction temperatures and types of coke, and the factors that influence these were also identified.

EXPERIMENTAL METHOD

1. Coke Reactivity Test Apparatus (CRTA)

Fig. 1 shows a schematic of the CRTA used for the coke gasification experiment. This equipment is comprised of a furnace section for heating, a reactor section for conducting the coke gasification

[†]To whom correspondence should be addressed.

E-mail: chjeon@pusan.ac.kr

Copyright by The Korean Institute of Chemical Engineers.

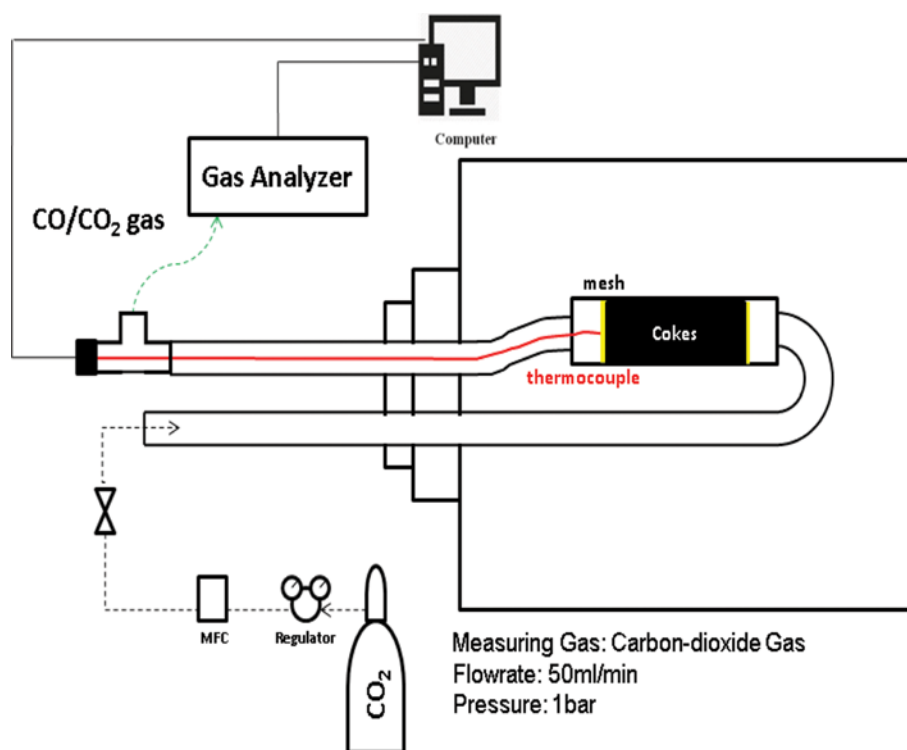


Fig. 1. Schematic of CRTA.

reaction by supplying CO₂ gas, a thermocouple for measuring the coke reaction temperature, and a Thermo Scientific Nicolet 6700 FT-IR Spectrometer for measuring the CO gas after gasification. The

coke gasification reactor was cylindrically shaped with a diameter of 20 mm and length of 100 mm. The maximum temperature of the furnace and heating rate were 1,400 °C, and 30 °C/min, respec-

Table 1. Proximate, ultimate analysis, and ash composition of coal and coke

Coal		A	B	C	D	E	FX_raw	LT_raw	FX_coke	LT_coke
Proximate analysis (wt%, Asd basis)	Moi.	0.20	1.47	0.28	0.23	0.39	0.49	1.07	0.59	2.06
	V.M.	0.77	0.95	1.87	1.89	2.07	23.56	30.33	1.48	2.47
	Ash	12.32	13.03	10.56	10.44	10.57	10.26	8.49	14.03	13.82
	F.C.	86.71	84.55	87.29	87.44	86.97	65.7	60.11	83.90	81.65
Ultimate analysis (wt%, daf basis)	C	86.64	84.43	96.12	94.57	96.91	80.92	77.27		
	H	0.88	0.67	0.69	0.56	0.42	6.11	5.10		
	O	-	-	1.84	3.46	1.21	11.29	16.13		
	N	0.63	0.75	0.92	0.97	1.01	1.24	0.89		
	S	0.58	0.42	0.42	0.44	0.45	0.45	0.61		
Ash composition (wt%)	Na ₂ O	0.5	0.5	0.6	0.48	0.5	0.45	0		
	MgO	0.8	0.5	0.94	0.83	0.97	0.31	0.69		
	Al ₂ O ₃	23.6	20.5	22.17	22.34	22.51	27.44	24.45		
	SiO ₂	55.3	65.8	45.49	45.66	45.0	54.85	47.84		
	PO ₂	1.1	0.2	1.41	1.47	1.11	0.13	0.28		
	SO ₃	0.6	-	1.29	1.24	0.82	0.64	0.41		
	K ₂ O	1.5	1.4	2.38	2.34	2.48	1.89	4.87		
	CaO	3.9	1	6.7	6.32	5.78	2.5	2.97		
	TiO ₂	1.8	1.7	2.54	2.54	2.47	2.64	2.76		
	Fe ₂ O ₃	9.3	7.5	14.57	14.6	15.69	8.48	14.76		
etc	1.6	0.9	1.91	2.18	2.67	0.67	0.97			

tively. At 1 bar, the flow rate of CO₂ gas was 50 mL/min and the CO and CO₂ were measured after reacting with coke. Coke temperatures and post-reaction CO were measured and the measured data were saved in real time by connecting to a computer.

2. Thermogravimetric Analysis (TGA)

Thermogravimetric analysis (TGA) is capable of heating from room temperature (RT) to a peak temperature of 1,500 °C with heating rates of 100 °C/min up to 1,000 °C and 25 °C/min up to 1,500 °C. It can also supply a variety of gases including air, nitrogen, oxygen, helium, CO, and CO₂. In the experiment, the temperature was raised at a heating rate of 50 °C/min up to 850, 950, 1,050, and 1,150 °C, which represented the temperatures for measuring the reactivity of coke under optimal conditions. Afterwards, gasification was conducted with CO₂ reaction gas at constant temperature for 120 min.

3. Cokes and Coal Properties

Table 1 shows the results from proximate, ultimate, and ash composition analyses on the cokes and raw coals used in the present study. A to E are cokes, FX and LT are raw coals. Cokes A and B were used for an initial investigation of the coke gasification characteristics. Cokes C, D and E were made from FX and LT coals with different blending ratios. These cokes were used to investigate the gasification reaction in more detail. The cokes contained 0.2-1.47% moisture, 0.77-2.07% volatile matter, 10.26-13.03% ash, and 54.55-87.44% fixed carbon. FX and LT coals contained 23.56 and 30.33% volatile matter prior to carbonization, respectively; subsequent proximate analysis after 3 h of carbonization at 1,050 °C showed reduction in volatile matter to 1.48 and 2.47%, respectively, indicating that the carbonization process had taken place successfully.

4. Coking Process of Raw Coal and Experimental Method

An electric furnace was used to produce coke from the FX and LT coals. The coke samples were produced by reacting for 3 h at 1,050 °C and then pulverizing it to obtain the samples. The lab-scale coke making apparatus is shown in Fig. 2. The vessel was charged with approximately 5 g of a raw coal sample. Then, the 200 g load was added to the coal sample. The furnace was heated to 1,050 °C at a heating rate of 3 °C/min. When the furnace temperature reached 1,050 °C, the temperature was maintained for 3 h and then cooled to room temperature. During the coke making process, nitrogen gas was used.

Using the previously introduced CRTA equipment, cokes with particle sizes of 1.18 mm-1.30 mm were divided into two types (A

and B cokes), and samples (10 g each) were reacted with CO₂ gas at 850, 950, 1,050, and 1,150 °C. Afterward, their reactivity was measured by the amount of CO gas emitted. First, the furnace was heated to the target temperature with a heating rate of 20 °C/min. Once the temperature reached its target, the coke gasification reactor was inserted into the furnace. A thermocouple was used so that direct measurement of the coke particle temperature would be possible. When the coke particle temperature was reaching the target furnace temperature, CO₂ gas was flowed through the coke gasification reactor.

Coke reactivity was assessed using the JIS coke reactivity index (R_{cI}), which is different from the ASTM standard for the measurement of coke R_{cI}. The difference is that the ASTM standard stipulates coke reactivity through measurements of coke weight before and after the gasification reaction, whereas the JIS standard uses the concentration of the reacting gas to measure coke reactivity. The equation for coke R_{cI} measurement according to the JIS standard is shown in Eq. (1) below:

$$R_{cI} = \frac{CO}{CO + 2CO_2} \times 100 \quad (1)$$

Coke reactivity by the JIS standard was measured using the concentration of CO gas emitted from the gasification reaction with CO₂ gas supplied for gasification.

RESULTS AND DISCUSSION

1. Comparison between the Characteristics of Cokes A and B

1-1. Carbon Conversion and Reaction Rate

Fig. 3 shows the carbon conversion of cokes A and B from the temperature ramps in the TGA, while the reaction rates of cokes A and B are analyzed in Fig. 4. Regardless of the type of coke, an increase in temperature resulted in a faster carbon conversion. At 850 °C, cokes A and B showed almost no difference in carbon conversion, but the difference increased at 950 and 1,050 °C. At 1,150 °C, the two cokes showed no difference in carbon conversion again. In all cases, coke B had a faster carbon conversion than coke A. The reaction rate coefficients were used in the Arrhenius equation to calculate activation energies for the conversion of cokes A and B as 162.26 and 158.51 kJ/mol, respectively. In contrast, the activation

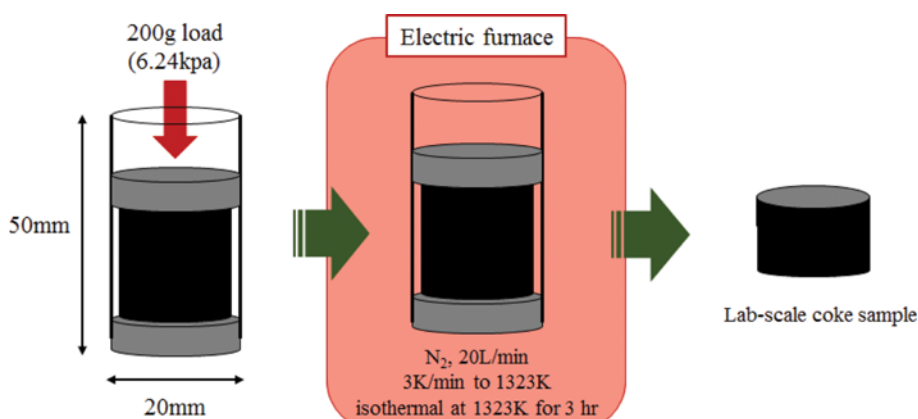


Fig. 2. Schematic of lab-scale coke making apparatus.

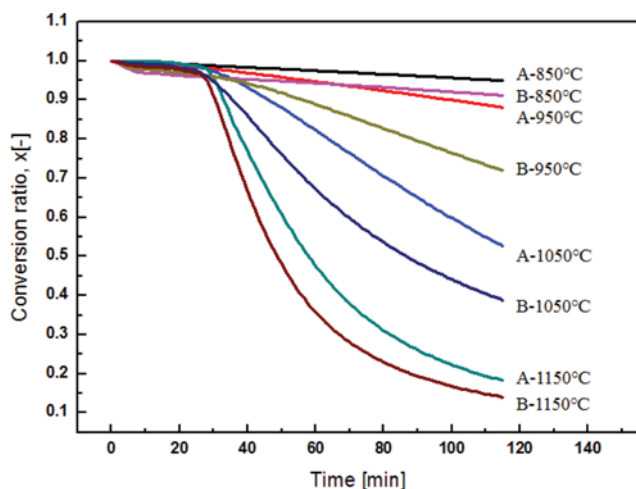


Fig. 3. Carbon conversion with time at different temperatures.

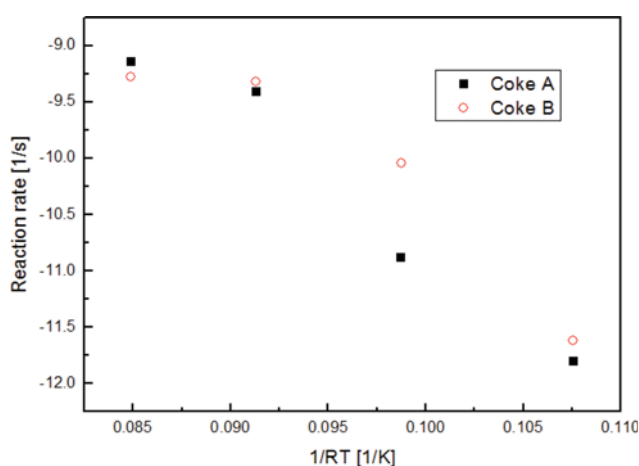


Fig. 4. Reaction rate of A and B cokes over temperature.

energies of petroleum and metallurgical coke with CO₂ gas reported by previous researches [16-19] were in the range 215-239 kJ/mol for reaction temperatures between 600 and 900 °C. These differences could be explained by three different 'regimes', reaction control (regime I), pore diffusion (regime II) and gas phase mass transfer (regime III). The previous research was usually conducted in the reaction control regime, whereas this study was conducted under both reaction control and pore diffusion with a transition temperature was found at 1,050 °C.

Surface area analysis via SEM images and BET measurements helped explain why coke B had higher reactivity. Porosity had developed the most at 950-1,050 °C regardless of coke type, while the specific surface area (SSA) was also greater in this temperature range than at other temperatures. Therefore, we believe that because coke B was more porous than coke A and had greater SSA, coke B showed higher reactivity. As coke underwent gasification, its reactivity was confirmed to change according to changes in temperature, porosity, and SSA.

1-2. CO Emission and Coke Reactivity Index (R_i)

To measure the CO emission generated from the CO₂ gasification

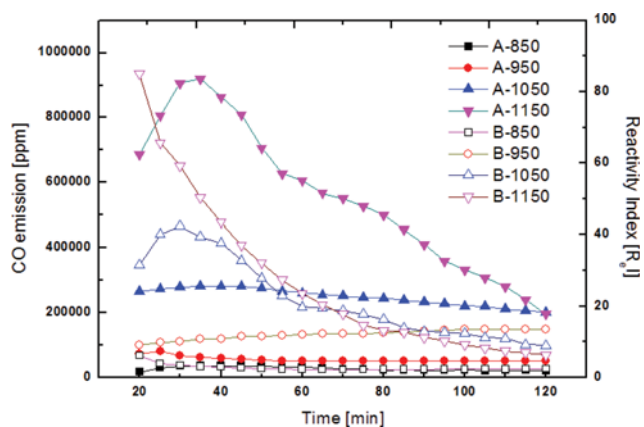


Fig. 5. CO emission and reactivity index over time at various temperatures.

reaction of coke, the CRTA and Thermo Scientific Nicolet 6700 FT-IR Spectrometer were used to measure CO gas. CO is the product generated from gasification between C (from coke) and CO₂. Fig. 5 shows the measurement results of CO gas emissions and the coke reactivity index for cokes A and B after CO₂ gasification at various times and temperatures. Regardless of coke type, CO emissions increased as the temperature increased. At a relatively low temperature of 850 °C for the experiment, the level of CO emissions from cokes A and B were nearly the same at approximately 27,000 and 30,000 ppm, respectively, which confirmed that despite their low reactivity, the cokes reacted uniformly and steadily. The levels of CO emission from coke B increased from 30,000 ppm at 850 °C to 150,000 ppm at 950 °C, while the reactivity of coke A remained nearly the same. At 1,050 °C, differences were found according to coke type, with coke A showing uniform CO emissions over time of approximately 280,000 ppm of CO emission, which was significantly higher than at 850 °C and 950 °C. Conversely, coke B showed peak emission of approximately 460,000 ppm after about 30 min of reaction time and continued to decrease thereafter, which could have been caused by a highly active reaction due to its high reactivity. When the temperature reached 1,150 °C, peak values in CO emission levels appeared regardless of coke type with cokes A and B generating 910,000 and 930,000 ppm, respectively. The peak emission occurred for coke A at ~35 min, whereas coke B showed a continuous decrease from early on, which could be caused by coke B actively reacting from the beginning of the reaction (i.e., the CO and CO₂ concentration change until 20 min). The CO emission increased at 1,050 and 1,150 °C because as the reaction temperature increased, the coke gasification reaction became more active due to increasing diffusion of CO₂ to particle pores. These findings were also confirmed by the SEM images and SSA results, where more pores developed as the reaction temperature increased especially in coke B compared to in coke A; as a result, the SSA increased as well. Since gasification with CO₂ could occur more readily in the numerous pores that had developed, the CO emission increased accordingly.

CO emission after the CO₂ gasification of coke was measured by coke reactivity based on R_i (JIS standard). The results showed that regardless of coke type, coke reactivity increased as temperature

increased. The coke reactivity assessment based on the JIS standard measures the level of CO and CO₂ gas emissions. At 850 °C, cokes A and B showed R_I of approximately 1.8 and 3.5, respectively. Coke B clearly had a higher R_I, but both types of coke showed constant reactivity even as the reaction time increased. At 950 °C, the reactivity approximately doubled relative to 850 °C, with R_I of 4.21 and 8.03 for cokes A and B, respectively; as earlier, emissions did not change even as the reaction progressed further. When the temperature reached 1,050 °C, cokes A and B showed high reactivity with R_I of 16.43 and 30.40, respectively, which was attributed to the increased SSA from the development of pores. However, an examination of the average R_I values over the entire reaction showed cokes A and B with average R_I of 14.24 and 17.30, respectively. These results could have originated from a rapid reaction in the early stages due to their high reactivity. Then the reaction showed down because of a decrease in the number of pores and SSA, thereby decreasing the overall reactivity.

1-3. SEM Images and Specific Surface Area (SSA) Results

Fig. 6 shows the mass loss rate and SSA as a function of carbon conversion. In addition, Fig. 7 shows SEM images of cokes A and B that were acquired before and after the reaction to observe pore development based on carbon conversion. The peak mass loss rates

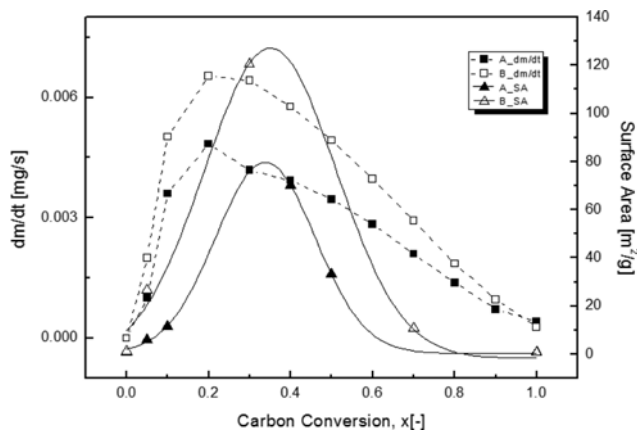


Fig. 6. Mass loss rate and specific surface area with carbon conversion of the cokes.

appeared when the carbon conversion ratio was approximately 0.2, with peak mass loss rates of 0.485 mg/s and 0.653 mg/s for cokes A and B, respectively, which indicated that coke B was faster by about 0.178 mg/s. As the carbon conversion and mass loss rate increased, coke A showed distinct pore development and an increase in the SSA from 0.7108 to 6.0338 m²/g. When carbon conversion was about 0.5, pore development reached its peak, and the SSA was also at its highest value of 33.1866 m²/g. Moreover, as the mass loss rate decreased, pore development gradually decreased, and the SSA decreased to 5.0166 m²/g. The surface of coke B became much smoother at a carbon conversion of 0.065 than before the reaction as the coke became less porous. However, the SSA of coke B at this point was 26.5420 m²/g, which indicated that the SSA had become larger than its initial value of 1.3061 m²/g prior to the reaction. Although the surface became smoother and appeared to lack pores, a maximum porosity developed at a carbon conversion of 0.308, which was a relatively low carbon conversion; at this point, the SSA was 120.5801 m²/g, a value that was about four-times higher than the maximum SSA of coke A. Consequently, the internal pores of coke B were more developed than the surface pores. With an increasing carbon conversion rate, CO₂ reacted with not only surface but also internal pores. The CO emissions and reactivities of coke A and B were not significantly different because most of the CO₂ reacted with the surface at lower carbon conversions. However, with increasing carbon conversion, coke B had high CO emission and reactivity because CO₂ easily reacted with both surface and internal pores due to increasing of diffusion. In summarizing the findings above, since proximate, ultimate, and ash analyses of cokes A and B showed similar results, similar reactivity may be expected between cokes A and B. As the reaction progressed, the SSA changed due to changes in porosity, which was believed to have affected the reactivity. Surface area measurements via Brunauer-Emmet-Teller (BET) theory showed that with both cokes A and B, the maximum SSA occurred at a carbon conversion of ~0.35. However, the SSA of B coke was about four-times higher than that of coke A (120.5801 versus 33.1866 m²/g). Considering that coke B had higher reactivity and SSA than coke A, pore development and the size of SSA had the greatest impact on coke reactivity compared to other factors used in the proximate, ultimate, and ash analyses.

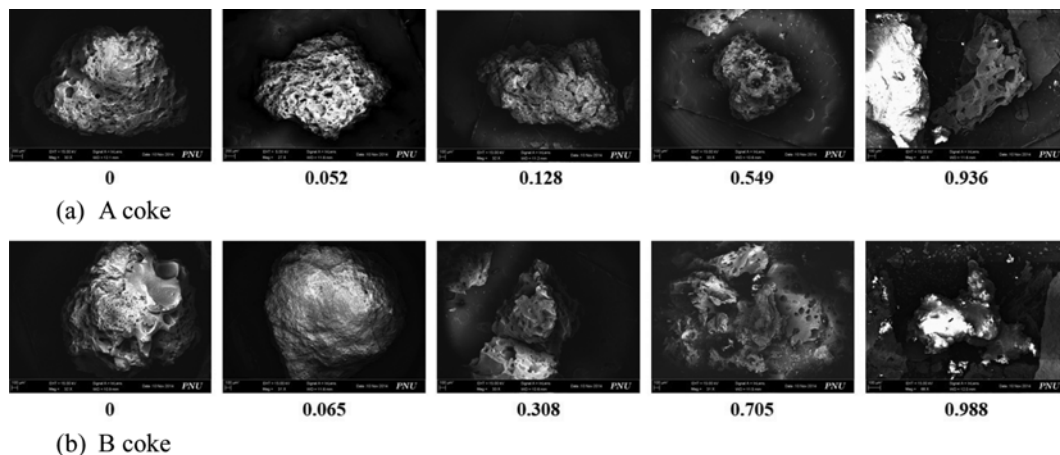


Fig. 7. SEM images of cokes at various carbon conversion.

2. Comparison of Reactivity According to Blending Ratios of Coals and Cokes C, D, and E

To analyze the gasification reaction of different cokes produced by varying only the blending ratio of FX and LT coals, cokes C, D, and E were used, along with FX and LT cokes produced by carbonization after adding 0, 30, 50, 70, and 100% LT coal relative to FX coal. The particle size was measured with an LS-13 320, which was a device with a high resolution limit and reproducibility designed for accurate differential measurement integrated with multiple wavelengths based on PIDS theory (a proprietary technology of Beckman Coulter), Fraunhofer diffraction, and Mie scattering theories. This device also has a wide particle distribution measurement range of 0.017-2,000 μm . Although the JIS standard recommends using particle sizes of 850-1.7 mm for the coke reactivity test, the experiment was conducted using samples with particle sizes of 1 mm and 1.18 mm to minimize the influence of particle size on the coke gasification reaction. While the cokes C, D, and E and FX coal had an average particle size of approximately 1,270 μm , LT coal had a slightly smaller particle size average of about 1,230 μm .

2-1. Carbon Conversion

For identification of carbon conversion via TGA, the cokes C, D, and E and cokes blended in ratios of 7:3, 5:5, and 3:7 with carbonized FX and LT, respectively, were used in the gasification reaction, as shown in Fig. 8. The order of carbon conversion over

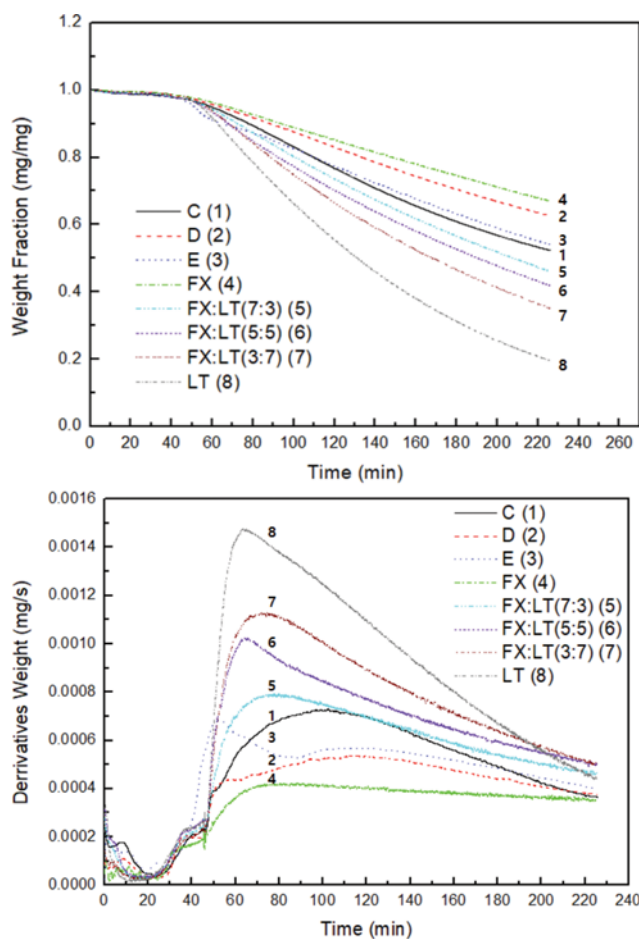


Fig. 8. Carbon conversion with time for different cokes.

time was $\text{LT} > \text{LT}:\text{FX}(7:3) > \text{LT}:\text{FX}(5:5) > \text{LT}:\text{FX}(3:7) > \text{C} > \text{E} > \text{D} > \text{FX}$. LT coal, which showed the highest reactivity, showed a peak mass loss rate of approximately 0.0015 mg/s, whereas FX coal, which showed the lowest reactivity, showed a peak mass loss rate of 0.004 mg/s, indicating a difference in reactivity of a factor of ~ 4 . Furthermore, a higher blending ratio of LT tended to improve the reactivity, and thus LT and FX coals played separate roles. LT coal showed significant pore development and a high SSA of 128.67 m^2/g , which created greater surface area for the reaction with CO₂ gas; however, as its reactivity increased its strength weakened. On the other hand, coke made from FX coal showed less pore development and its SSA was significantly smaller than LT coal at 36.45 m^2/g . For these reasons, the reactivity of FX coal was low, but its strength is expected to be high. The cokes C, D, and E were blended with a binder and had different carbonizing temperatures and densities, which made it difficult to compare these to FX and LT cokes produced without any binder. Regardless, their tendencies could be identified. Considering that carbon conversion occurred in the order of coke $\text{C} > \text{E} > \text{D}$, coke C was likely to have been blended with the highest ratio of LT coal, whereas coke D was likely to have been blended with the highest ratio of FX coal.

Fig. 9 shows the predicted blending ratios of FX and LT coals in cokes C, D, and E. The results of coke carbon conversion based on the blending ratios of FX and LT coals were used to predict the blending ratios of FX and LT coals used to produce cokes C, D, and E. Based on those results, the FX:LT blending ratios of cokes C, D, and E were predicted to be about 70:30, 90:10, and 75:25, respectively. As mentioned, the production conditions of the binder and cokes may be different from the actual production conditions, but the study was able to analyze only the effects of the FX and LT coals.

2-2. CO Concentration and Reactivity of Cokes C, D, and E and FX and LT Coal Blending Ratios

Fig. 10 shows the CRTA results of CO concentrations and reactivity values of cokes C, D, and E and different blending ratios of FX and LT after gasification. The average concentration of CO gas after gasification appeared in the order $\text{C} > \text{E} > \text{D}$. The maximum concentrations of CO from the cokes C, D, and E over the entire

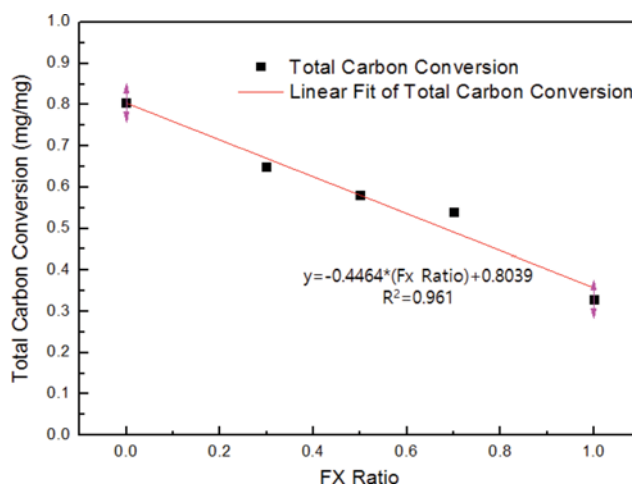


Fig. 9. Effect of FX blending ratio on carbon conversion.

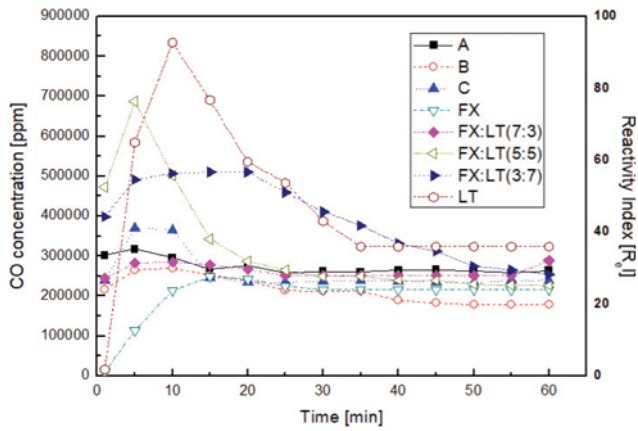


Fig. 10. CO concentration with time for cokes C, D, E and different blending ratios of FX and LT.

reaction time were approximately 320,000, 280,000, and 400,000 ppm, respectively, appearing in the order E>C>D. However, the average concentrations of CO from cokes C, D, and E over the entire reaction time were approximately 280,000 ppm, 210,000 ppm, and 250,000 ppm, respectively, appearing in the order C>E>D. Because reactivity according to the JIS standard is also analyzed based on

CO concentrations, the maximum reactivities of cokes C, D, and E were approximately 19, 16, and 23, respectively, also in the order E>C>D. In contrast, the average reactivity of cokes C, D, and E was approximately 16, 12, and 15, respectively, in the order C>E>D, which was consistent with the CO concentration results. The maximum and average CO concentrations and reactivities demonstrated that cokes C and E had similar CO concentrations and reactivity results. Such similar results were likely to be caused by the same phenomena since cokes C and E were produced with similar FX and LT blending ratios of 70 : 30 and 75 : 25, respectively.

The maximum CO gas concentrations appeared in the order LT>LT:FX(5:5)>LT:FX(7:3)>LT:FX(3:7)>FX, while the average CO concentrations appeared in the order LT>LT:FX(7:3)>LT:FX(5:5)>LT:FX(3:7)>FX. In the first 5 min of the reaction, the CO concentration of FX:LT(5:5) was the highest but tended to decrease with time. The average CO concentrations showed that the concentrations increased as the blending ratio of LT coal increased. The reactivity results were also consistent with the characteristics of CO concentrations. In this case, the CO₂ gasification reaction was facilitated by penetration into the pores that had become wider, leading to increased CO concentration (reactivity).

2-3. SEM Images and SSA Analysis

Fig. 11 shows the SEM images acquired before and after the

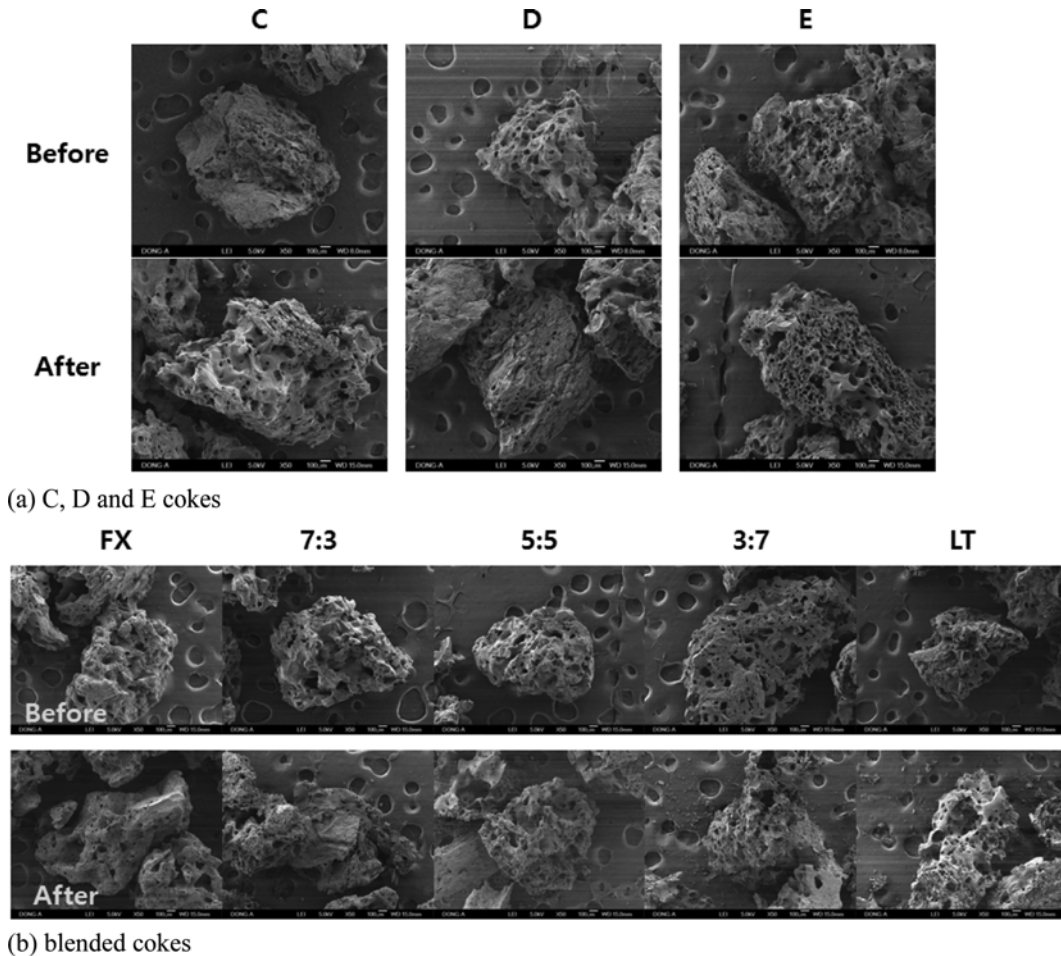


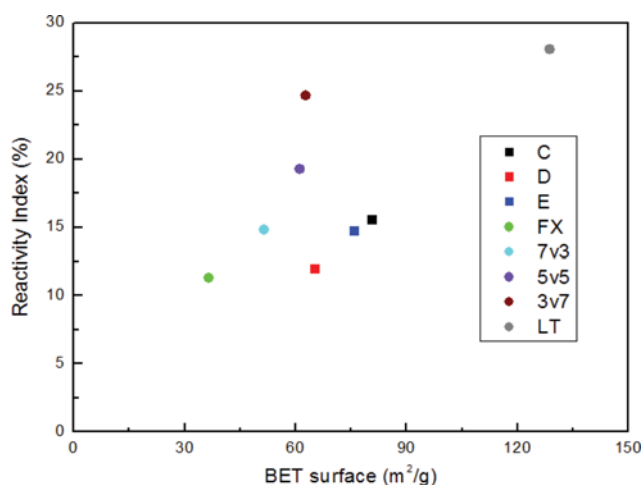
Fig. 11. SEM images of cokes before and after gasification.

Table 2. Specific surface area and density of the cokes (before the gasification reaction)

Coke	C	D	E	FX	LT
Specific surface (m ² /g)	1.03	1.07	1.09	10.93	43.24
Density (g/cm ³)	1.8880	1.8928	1.8838	1.9310	1.9286

gasification reaction with cokes C, D, and E and cokes blended with FX and LT coals. Tables 2 and 3 show the SSA and density results before and after the gasification reaction, while Fig. 12 shows the SSA and reactivity results. The results confirmed that more pores were present after the gasification reaction than before the reaction. Pore development in LT coke was especially prominent, where its SSA was the largest. FX coke showed slow pore development and had the smallest SSA with a smooth surface. These findings were consistent with the reactivity results mentioned earlier and the SSA results via BET also showed a similar pattern. Because FX coal has low reactivity, coke blended with a high amount of FX coal is expected to have reduced reactivity but greater strength, whereas an increased blending ratio of LT coal is predicted to reduce strength but improve reactivity. Therefore, it is important to find the appropriate blending ratio of coal that can form the basic structure and the coal that can enhance reactivity.

Tables 4 and 5 show the EDS results. Before gasification, only C, O, Al, and Si were detected in the coke samples, but after the reac-

**Fig. 12. Reactivity Index (Rel) relative to BET surface area.**

tion, Ca and Fe were also detected in the cokes. Catalytic substances such as Ca and Fe were detected in cokes with good reactivity, and higher reactivity was associated with higher Ca and Fe contents. A rapid increase in CO concentration was found in LT and LT:FX (5:5) in the first 15 min of the gasification reaction, which was attributed to a transient increase in coke gasification reactivity from catalytic effects. As the reaction progressed, the order of CO con-

Table 3. Specific surface area and density of the cokes (after the gasification reaction)

Coke	C	D	E	FX	FX:LT 70:30	FX:LT 50:50	FX:LT 30:70	LT
Specific surface (m ² /g)	80.64	65.07	75.79	36.45	51.42	61.09	62.70	128.67
Density (g/cm ³)	1.9706	1.9796	1.9777	1.9454	1.9954	1.9879	2.0039	2.0122

Table 4. EDS results before the gasification of cokes

C coke		D coke		E coke		FX		FX:LT			LT				
								7:3	5:5	3:7					
At%		At%		At%		At%		At%	At%	At%	At%				
C	90.99	C	91.51	C	93.33	C	90.68	C	91.36	C	91.35	C	91.46	C	83.71
O	8.37	O	6.43	O	5.99	O	8.19	O	7.85	O	7.83	O	7.20	O	14.68
Al	0.24	Al	0.94	Al	0.26	Al	0.42	Al	0.38	Al	0.35	Al	0.69	Al	0.68
Si	0.40	Si	1.12	Si	0.43	Si	0.71	Si	0.41	Si	0.46	Si	0.65	Si	0.93

Table 5. EDS results after the gasification of cokes

C coke		D coke		E Coke		FX		FX:LT			LT				
								7:3	5:5	3:7					
At%		At%		At%		At%		At%	At%	At%	At%				
C	88.13	C	88.97	C	90.33	C	82.39	C	79.79	C	77.62	C	60.90	C	53.81
O	10.36	O	9.99	O	8.60	O	10.80	O	14.90	O	18.81	O	31.50	O	37.72
Al	0.90	Al	0.34	Al	0.41	Al	2.99	Al	2.00	Al	1.10	Al	2.50	Al	2.41
Si	0.61	Si	0.70	Si	0.66	Si	3.82	Si	2.76	Si	1.06	Si	3.55	Si	2.68
								Fe	0.55	S	0.33	S	0.26	S	0.19
										Ca	0.61	Ca	0.28	Ca	0.88
										Fe	1.67	Fe	1.01	Fe	2.31

centration (reactivity) was determined proportional to be the SSA size. In summarizing the results from the present study and earlier studies [13,14], overall reactivity in the gasification reaction may have been determined by the size of SSA, but reactivity could increase due to the catalytic effects of Ca and Fe at early stages in the gasification.

CONCLUSIONS

To investigate the coke reactivity inside blast furnaces, the present study measured CO gas generated after coke gasification reactions and measured the coke R_{I} based on the JIS standard.

(1) The gasification reaction experiment with cokes A and B was conducted at reaction temperatures of 850, 950, 1,050, and 1,150 °C. Similar reactivities, were found for both coke types at the relatively low temperature of 850 °C and the relatively high temperature of 1,150 °C; no major differences according coke type were found at 950 °C and 1,050 °C.

(2) When cokes produced with FX and LT coals and cokes C, D, and E were blended with a binder (with particle size in the range of 1-1.18 mm), undergoing gasification at 950 °C, the reactivity was found to be in the order C>E>D.

(3) FX and LT coals were carbonized to produce cokes, and gasification reactions were performed according to the blending ratios of those coals. In these reactions, the reactivity appeared in the order of LT>LT:FX(7:3)>LT:FX(5:5)>LT:FX(3:7)>FX. Based on these findings, it was predicted that A, B, and C cokes had FX:LT blending ratios of about 7:3, 9:1, and 7.5:2.5, respectively, when the effects of other additives and binder were excluded.

(4) The SSA results based on SEM images and BET showed that LT coal with high reactivity had the largest SSA, while FX coal had the smallest SSA. As the blending ratio of LT carbon increased, the SSA also increased, resulting in increased reactivity as well.

(5) Physical properties from proximate, ultimate, and ash analyses showed no major differences according to coke type or blending ratio, while significant differences in reactivity were found according to coke type. Based on these findings, it was determined that coke reactivity is influenced more by pore development in cokes rather than their physical properties.

REFERENCES

1. Y. J. Cho, J. H. Kim, R. G. Kim, G. B. Kim and C. H. Jeon, *Trans. Korean Soc. Mech. Eng. B*, **38**, 807 (2014).
2. S. H. Yoon, Y. C. Choi, S. H. Lee and J. G. Lee, *Korean J. Chem. Eng.*, **24**, 512 (2007).
3. S. H. Lee, K. B. Choi, J. G. Lee and J. H. Kim, *Korean J. Chem. Eng.*, **23**, 576 (2006).
4. W. Yang, C. K. Ryu, S. M. Choi, E. S. Choi, D. W. Ri and W. W. Huh, *Trans. Korean Soc. Mech. Eng. B*, **28**, 747 (2004).
5. R. J. Gray and K. F. Devanney, *Int. J. Coal Geol.*, **6**, 277 (1986).
6. A. Cheng, *Iron and Steelmaker*, **28**, 39 (2001).
7. A. Cheng, *Iron and Steelmaker*, **28**, 26 (2001).
8. J. Price, J. Gransden and K. Hampel, 3rd McMaster Cokemaking Course, Vol. 1, Lecture No. 3, McMaster University, Hamilton, Ontario, Canada (2003).
9. A. Cheng, *Iron and Steelmaker*, **28**, 30 (2001).
10. A. K. Biswas, *Principles of Blast Furnace Ironmaking: Theory and Practice*, Cootha Publishing House, Brisbane, Australia, ISBN 0-949917-00-1, ISBN 0-949917-08-7 (1985).
11. R. Loison, P. Foch and A. Boyer, *Coke Quality and Production*, Second edition, Butterworths Borough Green, Sevenoaks Kent TN15 8PH, England, ISBN 0-408-02870-X (1989).
12. A. Cheng, *Iron and Steelmaker*, **28**, 78 (2001).
13. J. D. Yang, A. McLean and I. D. Sommerville, *Iron and Steelmaker*, **27**, 103 (2000).
14. M. Grigore, R. Sakurovs, D. French and V. Sahajwalla, *Energy Fuels*, **23**(4), 2075 (2009).
15. B. Gao, J. L. Zhang, H. B. Zuo, C. L. Qi, Y. Rong and Z. Wang, *J. Iron. Steel Res. Int.*, **21**, 723 (2014).
16. N. M. Laurendeau, *Prog. Energy Combust. Sci.*, **4**, 221 (1978).
17. M. Kawakami, Y. Mizutani, T. Ohyabu, K. Murayama, T. Takenaka and S. Yokoyama, *Steel Res. Int.*, **75**, 84 (2004).
18. B. Y. Pang, R. J. Harris, R. J. Tyler and R. J. Sakurovs, *Thirteenth Annual International Pittsburg Coal Conference Proceedings*, **1**, 506 (1996).
19. D. J. Harris and I. W. Smith, *Symposium (International) on Combustion*, **23**, 1185 (1991).